Passive and dynamic gait measures for biped mechanism: formulation and simulation analysis

Carlotta Mummolo†‡ and Joo H. Kim†*

†*Department of Mechanical and Aerospace Engineering, Polytechnic Institute of New York University (NYU-Poly), Brooklyn, New York, USA*
‡*Department of Mechanical and Management Engineering, Polytechnic of Bari, Bari, Italy*

SUMMARY
Understanding and mimicking human gait is essential for design and control of biped walking robots. The unique characteristics of normal human gait are described as passive dynamic walking, whereas general human gait is neither completely passive nor always dynamic. To study various walking motions, it is important to quantify the different levels of passivity and dynamicity, which have not been addressed in the current literature. In this paper, we introduce the initial formulations of Passive Gait Measure (PGM) and Dynamic Gait Measure (DGM) that quantify passivity and dynamicity, respectively, of a given biped walking motion, and the proposed formulations will be demonstrated for proof-of-concepts using gait simulation and analysis. The PGM is associated with the optimality of natural human walking, where the passivity weight functions are proposed and incorporated in the minimization of physiologically inspired weighted actuator torques. The PGM then measures the relative contribution of the stance ankle actuation. The DGM is associated with the gait stability, and quantifies the effects of inertia in terms of the Zero-Moment Point and the ground projection of center of mass. In addition, the DGM takes into account the stance foot dimension and the relative threshold between static and dynamic walking. As examples, both human-like and robotic walking motions during single support phase are generated for a planar biped system using the passivity weights and proper gait parameters. The calculated PGM values show more passive nature of human-like walking as compared with the robotic walking. The DGM results verify the dynamic nature of normal human walking with anthropomorphic foot dimension. In general, the DGMs for human-like walking are greater than those for robotic walking. The resulting DGMs also demonstrate their dependence on the stance foot dimension as well as the walking motion; for a given walking motion, smaller foot dimension results in increased dynamicity. Future work on experimental validation and demonstration will involve actual walking robots and human subjects. The proposed results will benefit the human gait studies and the development of walking robots.

KEYWORDS: Biped system; Dynamic gait measure (DGM); Optimization; Passive dynamic walking; Passive gait measure (PGM); Passivity weight; Stability; Static walking; Zero-moment point (ZMP).

Nomenclature

$^{i-1}\mathbf{A}_i$:	Homogeneous transformation matrix for two adjacent coordinate frames.
$^{0}\mathbf{p}_i$:	Position vector of the ith local frame in terms of the global frame.
$^{0}\mathbf{s}_i$:	Position vector of the ith point mass in terms of the global frame.
$^{j}\mathbf{R}_i$:	Rotation matrix between two local frames i and j.
$-T, T$:	Single support initial and final time instants respectively.
a:	Foot rear dimension.
b:	Foot front dimension.
c_i:	Ratio of distance of ith point mass from previous joint over the entire link length l_i.
$\bar{d}$:	Root mean square distance between ZMP and GCOM in x direction over one-step period.
$\bar{d}_{\text{lim}}$:	Root mean square distance between ZMP and GCOM_{lim}.
DGM:	Dynamic Gait Measure.
DS:	Double support.
DW:	Dynamic walking.
fh:	Foot height.
FSR:	Foot support region.
GCOM:	Ground projection of center of mass.
GCOM_{lim}:	Maximum GCOM displacement within FSR.
J:	Cost function for optimization.
K:	Least upper bound of DGM value.
l_i:	ith link's length.
l_t:	Distance of torso mass m_2 from the pelvis.
$\dot{L}_{z,i}$:	Time rate of change of angular momentum of ith link about its COM.
mhi:	Malleolus position of rear foot at initial time instant $-T$.
m_i:	ith point mass.
PGM:	Passive Gait Measure.
sh:	Step height at mid-stance.
sl:	Step length.
SS:	Single support.
SW:	Static walking.
v:	Walking speed.

* Corresponding Author. E-mail: jhkim@poly.edu

w_i: Weight function.

x_i, y_i: x, y coordinates of ith joint, respectively, in terms of the global frame.

$\bar{x}_i, \bar{y}_i$: x, y coordinates of ith link's COM, respectively, in terms of the global frame.

ZMP: Zero moment point.

$\alpha_i, \beta_i, \gamma_i, \delta_i$:   Coefficients of polynomial functions.

θ_i: Generalized coordinates for ith joint angle.

$\tau_{i,max}$:   Maximum actuator torque for ith joint.

$\bar{\tau}_1$:   Root mean square value of the stance ankle torque.

$\bar{\tau}_{tot}$:   Root mean square value of the total actuation.

τ_i: Generalized torque for ith joint.

1. Introduction

Mechanical principles of biped walking have been studied by many researchers for a long time, and are still one of the active subjects in the field of robotics and biomechanics.[1,2] Researchers investigate locomotion of humans and other animals when designing robots whose motion and physical construction mirror those of living things. The balance and dynamics of walking, hopping, and running have been studied extensively in biomechanics in order to gain a better understanding of human and animal locomotion. The human body with its limbs, head, and torso forms a well-balanced walking machine that performs periodic and energy-efficient gait. For this reason, the development of humanoid robots tends to mimic humans' performance in terms of design and motion control. As a consequence, such biped robots are one of the major topics of robotics research, which also have high potentials for future applications.

Human locomotion is a controlled and complicated process, but to analyze its dynamics, investigating simpler systems is essential. Various simplified biped models have been introduced in the literature.[1] The most widely accepted is the Inverted Pendulum Model (IPM[3]; Fig. 1) that exploits the simple inverted pendulum analogy. The IPM proposes that it is mechanically beneficial for the stance leg to behave like an inverted pendulum, prescribing a circular arc for the center of mass (COM) located at the hip.[4] Although many other different theories have been developed,[1,3–5] the IPM serves as a basis for many recent gait models. More advanced models have been developed based on the IPM to generate human-like trajectories, such as TMIPM[6] (Fig. 1), GCIPM,[7] MMIPM[8] (Fig. 1), 3DLIPM,[9] and PIPM.[10]

The inverted pendulum analogy is usually adopted for systems that perform Dynamic Walking (DW), in which the motion is largely dictated by the passive dynamics of the limbs. It requires minimal actuation to sustain the periodic behavior of the gait.[4] The motion of a dynamic walker is influenced significantly by the gravitational and inertial characteristics of the system, rather than being imposed by the controller.[11] Research work on DW focuses on different types of walkers; these can be divided into unactuated (fully passive) walkers[12] and actuated walkers, such as efficient actuator-assisted walkers[13,14] and actuated limit cycle walkers.[15,16] The passive dynamic walking principle was originally introduced by McGeer,[12] where the simple passive dynamic walker can walk down a slope with no controlled actuation, but under the power of gravity alone; it has been demonstrated that some anthropomorphic legged mechanisms exhibit stable, human-like walking on a range of shallow slopes, with no controlled actuation. McGeer's work[12] inspired many researchers who used the passive dynamic walker as a starting point to build walking robots that are mainly passive, but minimally actuated in order to walk on level ground.[17,18] For instance, Collins *et al.*[13] presented passive dynamic walkers which can walk on level ground with small active power sources in substitution of gravity. Using a natural dynamics-based control rather than a model-based trajectory control, their robot results in a very natural human-like gait with less energy consumption.[14] Also, it has been found that humans try to correct any tendency to fall during normal walking while minimizing the energy consumption rather than following a specific trajectory for global progression.[5] Similarly, the DW of robots is not dictated substantially by the controller, but is rather determined by the natural limb dynamics.[11]

Unlike passive dynamic walking robots, some other models are developed for active control based on Zero Moment Point (ZMP). The ZMP is the point on the foot/ground contact surface where the net ground reaction forces are applied, while the tipping moment – the tangential component of the ground reaction moment – is zero.[19] The Foot Support Region (FSR; also called support base, stability region, foot contact area, etc.) is delimited by the points of the system in contact with the ground, which corresponds to the surface of the convex hull linking the contact points together. The ZMP must always reside within the FSR, and whenever the calculated ZMP falls outside this region, it should be an indication of non-physical behavior.[20] The concept of the ZMP is useful in understanding dynamic stability and also for monitoring and controlling walking robots.[21] To ensure dynamic stability based on the ZMP, usually an ideal trajectory for ZMP is planned and followed by a feedback controller,[22] resulting in unnatural gaits with inefficient locomotive actuation. However, the ZMP control approach is useful for robotic gait with varying walking speeds (v) and step sizes.[23]

In contrast to DW, the gait is called Static Walking (SW) if the ground projection of the center of mass (GCOM) stays within the FSR to maintain static stability.[24] However, SW, usually performed by humanoid robots, results in unnatural motion with low speed (0.15–0.4 m/s) and small step length (sl; 0.2–0.5 m).[6,8,22,25] It is known that natural human gaits are generally not stable statically, but typically consist of phases in which the GCOM leaves the FSR, while the dynamics and the momentum of the segments are used to keep the gait dynamically stable, i.e., ZMP is kept inside the FSR.[19,20,26]

Actual robotic biped systems, as well as humans, are much more articulated than the IPM. Thus, the motion generation and control problems of biped walking usually include kinematic and actuation redundancies. To resolve the redundancy, optimization methods have been widely used in the literature where various cost functions are introduced, such as energy consumption, actuator torques ($\boldsymbol{\tau}_i$), reference trajectory error, and their combinations.[1,2,27−36]

Inverted pendulum model of walking
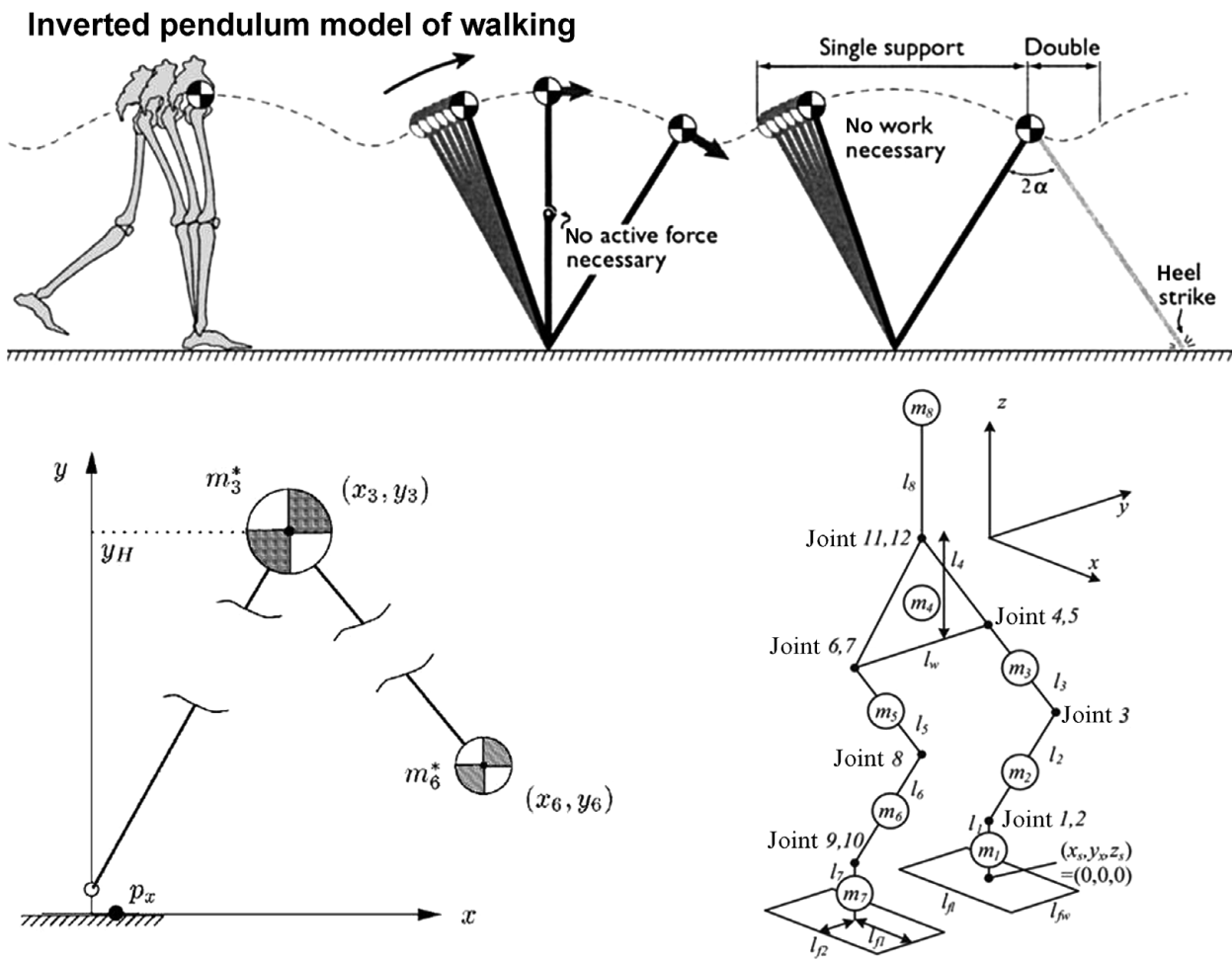
Fig. 1. Simple walking models based on inverted pendulum – IPM (top[3]), TMIPM (bottom left[6]), and MMIPM (bottom right[8]).

As seen in the broad literature as above, the natural human walking is characterized as "passive" and "dynamic." Passivity is associated with the actuation control, while dynamicity is associated with static equilibrium. However, normal human walking is neither fully passive nor constantly dynamic, and the quantification of the level of passivity and dynamicity has not been rigorously investigated in the literature. In this paper, we propose initial formulations of quantitative mechanical measures of passivity and dynamicity of biped walking, based on the aforementioned scientific motivations. The passivity is consistent with the optimality of natural walking, where the gait is generated by minimizing physiologically inspired weighted actuator torques. The passivity is described in terms of the relative contribution of the stance ankle actuator torque. The dynamicity is associated with the gait stability, where the inertia effect is represented in term of the ZMP and GCOM. Using this approach, both human and robotic walking motions with various stance foot dimensions are generated for comparison, physical interpretations, and proof-of-concept demonstrations. The introduction and demonstration of such initial concepts through computer simulation in this research will provide theoretical foundations for future experimental validation of the proposed measures. This study will eventually provide valuable insights in exploring and understanding fundamental principles of human biped walking. The proposed measures can also be used as criteria for design and control of walking robots.

In the next section, the kinematic and dynamic models of a planar biped system are explained, followed by the description of the gait model used in the current problem. Next, the gait stability in terms of the GCOM and the ZMP is described, and the Dynamic Gait Measure (DGM) is defined. Then optimization problem is formulated along with passivity weights-based actuation cost function inspired by physiologic human energy consumption. The Passive Gait Measure (PGM) is then introduced. Numerical results of biped walking for human and robot will be demonstrated and analyzed with the measures of optimality, passivity, and dynamicity, followed by a discussion about the future work on experimental validation.

2. Biped System Model and Dynamics
For the purpose of this research as described earlier, we focus on one step, single support (SS) phase during the periodic motion of biped walking. Therefore, the impulse at the heel contact is not considered in formulating the dynamics. The SS phase analysis is identified in this research because the passivity and dynamicity in the double support (DS) phase are not as important as in the SS phase due to its relatively short duration[37] and less dynamic nature – usually both GCOM
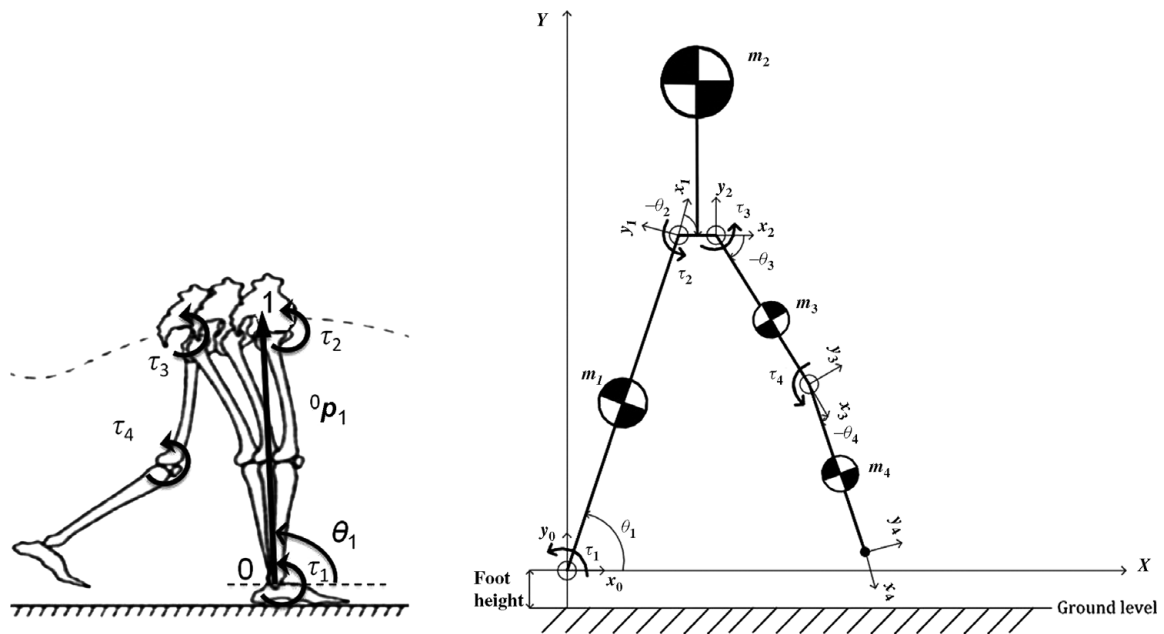
Fig. 2. Biped system in the sagittal plane.

and ZMP exist within the FSR;[20] this is also consistent with many SS phase models described earlier.[37] For simplicity, a two-dimensional (2D) planar biped system is modeled where the motion is confined in the sagittal plane (Fig. 2). Generally, both the passive and dynamic nature of biped walking is most significant in the sagittal plane compared with those in the frontal plane. Since the main progression of normal walking occurs in the sagittal plane with major momentum in the forward walking direction, the range of lateral motion and the variance of the GCOM in the frontal plane are much smaller than that in the sagittal plane. In fact, it has been shown that the displacements of the GCOM and the ZMP in the frontal plane during normal human walking are very small compared with those in the sagittal plane.[20,38] Furthermore, the lateral movement during normal walking has negligible effect on the sagittal plane motion and it is usually assumed that the two-plane motions are decoupled due to, for instance, the minor pelvic sway motion[17] (approximately 4° [8,52]), and very small coupled (vertical) displacements.[10] For this reason, many other gait models in the literature as seen above have been analyzed in the sagittal plane,[10,17] which is consistent with our proposed approach and validates its feasibility.

The proposed model can be regarded as an extension of the concept of the IPM to a multiple-masses model in which the stance foot is assumed to be in a fixed full contact with the ground, while the hips and the upper body act like an inverted pendulum. While modeling the role of the foot, particularly the changes of the ankle position during the SS phase with full foot and toe contacts, can provide detailed gait realization, one benefit of using a simplified model, as in this case, is that the underlying principles and the physical interpretations can be demonstrated and analyzed rather directly for proof-of-concepts. For this reason, as described previously, many gait research work in the literature used various simplified models based on the full foot contact assumption without detailed foot movement or minor change in ankle positions during SS; examples include IPMs and their extensions,[6–8,26]

which is consistent with our proposed model. In particular, more explicit assumptions on the full foot contact during SS phase can be found in the literature.[17,39] In addition, this assumption is shown to be valid from kinematic gait data[40] indicating that the stance foot ankle position change occurs in a short time duration (10% of the total gait cycle) and its height increases by a very small amount (e.g., approximately 3 cm from the full foot contact initial position to the toe contact final position at the end of the SS phase). The biped system is a four-link kinematic open-loop chain with four revolute joints and four point masses:

- Link 1 represents the stance leg, which has length l_1 and is pinned at the ankle joint during SS. The point mass m_1 represents the leg's total mass. The stance leg is modeled as a single rigid body, since the knee angle is almost constant during most of the SS phase and its flexion is typically very small.[30,38]
- Link 2 represents the upper body that connects the two legs, where the distance between the hip joints l_2 should be zero in the sagittal plane (for modeling purpose in this paper, a very small length is assigned for l_2). The total upper body mass m_2 includes the head, the torso, and the arms, and its COM is located at a distance l_t above the pelvis.
- Links 3 and 4 represent the upper and lower swinging legs, with point mass m_3 and m_4 respectively.

The link lengths and the mass distribution have been chosen according to human anthropometry data[38] (Table I). The point masses are located at each link's COM, and thus the inertial parameters (mass and moments/products of inertia) in terms of the Denavit–Hartenberg local coordinate frame provide reasonable approximations for the joint-space dynamics (described below), particularly within the given ranges of momentum and inertia for normal walking. This approach is also in line with many robotic and human walking

Table I. Model parameters of proposed biped system[38].

Link	Name	Length (m)	Mass (kg)	c_i
1	Stance leg	0.90	13.9	0.674
2	Hip + torso (l_t)	0.01 + 0.4	47.2	0.5
3	Thigh	0.43	10.6	0.445
4	Shank	0.47	3.3	0.405

models in the literature, where the point mass assumption is shown to be valid[6,41,42] and widely adopted[6–9,43].

The global and local reference frames for each link are attached and the mechanism's 4 degrees of freedom (DoF), θ_1, θ_2, θ_3, θ_4, are represented according to the standard Denavit–Hartenberg kinematic convention (Fig. 2). The global reference frame is located at the ankle joint of the stance foot. The 4×1 position vector of each link's end point in terms of the global frame can be calculated using homogeneous transformation as follows:

$$^0\mathbf{p}_i = {}^0\mathbf{A}_1 \ldots {}^{i-1}\mathbf{A}_i {}^i\mathbf{p}_i \quad (i = 1, 2, 3, 4), \quad (1)$$

where $^{i-1}\mathbf{A}_i$ is the 4×4 homogeneous transformation matrix for two adjacent coordinate frames in terms of the Denavit–Hartenberg parameters,[44] which can be simplified for our model as follows:

$$^{i-1}\mathbf{A}_i(\theta_i) = \begin{bmatrix} \cos\theta_i & -\sin\theta_i & 0 & l_i\cos\theta_i \\ \sin\theta_i & \cos\theta_i & 0 & l_i\sin\theta_i \\ 0 & 0 & 1 & 0 \\ 0 & 0 & 0 & 1 \end{bmatrix}. \quad (2)$$

Then the global position x- and y-coordinates of each end point are as follows (in this paper, $^0\mathbf{p}_i$ is used to represent either 4×1 or 2×1 vector, depending on the context):

$$\text{Stance leg hip, } {}^0\mathbf{p}_1 = \begin{bmatrix} x_1 \\ y_1 \end{bmatrix} = \begin{bmatrix} l_1\cos\theta_1 \\ l_1\sin\theta_1 \end{bmatrix},$$

$$\text{Swing leg hip, } {}^0\mathbf{p}_2 = \begin{bmatrix} x_2 \\ y_2 \end{bmatrix} = \begin{bmatrix} l_1\cos\theta_1 + l_2\cos(\theta_1+\theta_2) \\ l_1\sin\theta_1 + l_2\sin(\theta_1+\theta_2) \end{bmatrix},$$

$$\text{Swing leg knee, } {}^0\mathbf{p}_3 = \begin{bmatrix} x_3 \\ y_3 \end{bmatrix} = \begin{bmatrix} l_1\cos\theta_1 + l_2\cos(\theta_1+\theta_2) + l_3\cos(\theta_1+\theta_2+\theta_3) \\ l_1\sin\theta_1 + l_2\sin(\theta_1+\theta_2) + l_3\sin(\theta_1+\theta_2+\theta_3) \end{bmatrix},$$

$$\text{Swing leg ankle, } {}^0\mathbf{p}_4 = \begin{bmatrix} x_4 \\ y_4 \end{bmatrix} = \begin{bmatrix} l_1\cos\theta_1 + l_2\cos(\theta_1+\theta_2) + l_3\cos(\theta_1+\theta_2+\theta_3) + l_4\cos(\theta_1+\theta_2+\theta_3+\theta_4) \\ l_1\sin\theta_1 + l_2\sin(\theta_1+\theta_2) + l_3\sin(\theta_1+\theta_2+\theta_3) + l_4\sin(\theta_1+\theta_2+\theta_3+\theta_4) \end{bmatrix}.$$

$$(3)$$

Here the trajectory of the stance leg hip ($^0\mathbf{p}_1$) is a circular arc of radius l_1, similar to the IPM. The positions of the point masses ($^0\mathbf{s}_i$) can be obtained in a similar way as follows:

$$^0\mathbf{s}_i = {}^0\mathbf{A}_i\bar{\mathbf{s}}_i \quad (i = 1, 2, 3, 4), \quad (4)$$

where $\bar{\mathbf{s}}_i$ is the local position of the COM of link i expressed in terms of ith local frame. The time derivatives, such as velocities and accelerations, are calculated using forward iteration starting from the ground (link 0), which has the velocity and acceleration under the gravitational field as $\boldsymbol{\omega}_0 = \dot{\boldsymbol{\omega}}_0 = \boldsymbol{v}_0 = \mathbf{0}$ and $\dot{\boldsymbol{v}}_0 = (0, g, 0)^T$.

The dynamics of the biped system is modeled using the recursive Newton–Euler equations of motion.[44] The actuator

torque $\boldsymbol{\tau}_i$ acting on the ith link is calculated as the axial component of moment $\mathbf{n}_i$ exerted on link i by link $i-1$, as follows:

$$\tau_i = \left({}^i\mathbf{R}_0\mathbf{n}_i\right)^T \left({}^i\mathbf{R}_{i-1}\mathbf{z}_0\right), \quad (5)$$

where $^j\mathbf{R}_i$ is the rotation matrix between two local frames i and j, and $\mathbf{z}_0 = (0, 0, 1)^T$. The moment term is calculated using backward iteration as follows:

$$^i\mathbf{R}_0\mathbf{n}_i = {}^i\mathbf{R}_{i+1}\left[{}^{i+1}\mathbf{R}_0\mathbf{n}_{i+1} + \left({}^{i+1}\mathbf{R}_0{}^0\mathbf{p}_i\right) \times \left({}^{i+1}\mathbf{R}_0\mathbf{f}_{i+1}\right)\right]$$
$$+ \left({}^i\mathbf{R}_0{}^0\mathbf{p}_i + {}^i\mathbf{R}_0\bar{\mathbf{s}}_i\right) \times \left({}^i\mathbf{R}_0\mathbf{F}_i\right) + {}^i\mathbf{R}_0\mathbf{N}_i, \quad (6)$$

$$^i\mathbf{R}_0\mathbf{f}_i = {}^i\mathbf{R}_{i+1}\left({}^{i+1}\mathbf{R}_0\mathbf{f}_{i+1}\right) + {}^i\mathbf{R}_0\mathbf{F}_i,$$

where

- $\mathbf{f}_i$ is the force exerted on link i by link $i-1$ at the origin of local frame $i-1$ to support link i and the links above;
- $\mathbf{F}_i$ is the total external force exerted on link i at the COM. Thus, referring to its own coordinate system, Newton's equation is $^i\mathbf{R}_0\mathbf{F}_i = m_i{}^i\mathbf{R}_0\bar{\mathbf{a}}_i$, where $\bar{\mathbf{a}}_i$ is the linear acceleration of the COM of link i. The linear velocity $\mathbf{v}_i$ of link i COM, the angular velocity $\boldsymbol{\omega}_i$ of link i, and the accelerations are calculated using the following forward iterative kinematic equations:

$$^i\mathbf{R}_0\bar{\mathbf{a}}_i = \left({}^i\mathbf{R}_0\dot{\boldsymbol{\omega}}_i\right) \times \left({}^i\mathbf{R}_0\bar{\mathbf{s}}_i\right) + \left({}^i\mathbf{R}_0\boldsymbol{\omega}_i\right)$$
$$\times \left[\left({}^i\mathbf{R}_0\boldsymbol{\omega}_i\right) \times \left({}^i\mathbf{R}_0\bar{\mathbf{s}}_i\right)\right] + {}^i\mathbf{R}_0\dot{\mathbf{v}}_i,$$

$$^i\mathbf{R}_0\dot{\mathbf{v}}_i = \left({}^i\mathbf{R}_0\dot{\boldsymbol{\omega}}_i\right) \times \left({}^i\mathbf{R}_0{}^0\mathbf{p}_i\right) + \left({}^i\mathbf{R}_0\boldsymbol{\omega}_i\right)$$
$$\times \left[\left({}^i\mathbf{R}_0\boldsymbol{\omega}_i\right) \times \left({}^i\mathbf{R}_0{}^0\mathbf{p}_i\right)\right] + {}^i\mathbf{R}_{i-1}\left({}^{i-1}\mathbf{R}_0\dot{\mathbf{v}}_{i-1}\right),$$

$$^i\mathbf{R}_0\dot{\boldsymbol{\omega}}_i = {}^i\mathbf{R}_{i-1}\left[{}^{i-1}\mathbf{R}_0\dot{\boldsymbol{\omega}}_{i-1} + \mathbf{z}_0\ddot{\theta}_i + \left({}^{i-1}\mathbf{R}_0\boldsymbol{\omega}_{i-1}\right) \times \mathbf{z}_0\dot{\theta}_i\right],$$

$$^i\mathbf{R}_0\boldsymbol{\omega}_i = {}^i\mathbf{R}_{i-1}\left[{}^{i-1}\mathbf{R}_0\boldsymbol{\omega}_{i-1} + \mathbf{z}_0\dot{\theta}_i\right]; \quad (7)$$

- $\mathbf{N}_i$ is the total external moment exerted on link i. The Euler's equation is $^i\mathbf{R}_0\mathbf{N}_i = ({}^i\mathbf{R}_0\mathbf{I}_i{}^0\mathbf{R}_i)({}^i\mathbf{R}_0\dot{\boldsymbol{\omega}}_i) + ({}^i\mathbf{R}_0\boldsymbol{\omega}_i) \times [({}^i\mathbf{R}_0\mathbf{I}_i{}^0\mathbf{R}_i)({}^i\mathbf{R}_0\boldsymbol{\omega}_i)]$, where $\mathbf{I}_i$ is the inertia matrix of link i about its COM with reference to the global frame.

Since no applied load other than the gravity is considered in the current problem, the backward iteration with $i = 4, \ldots, 1$
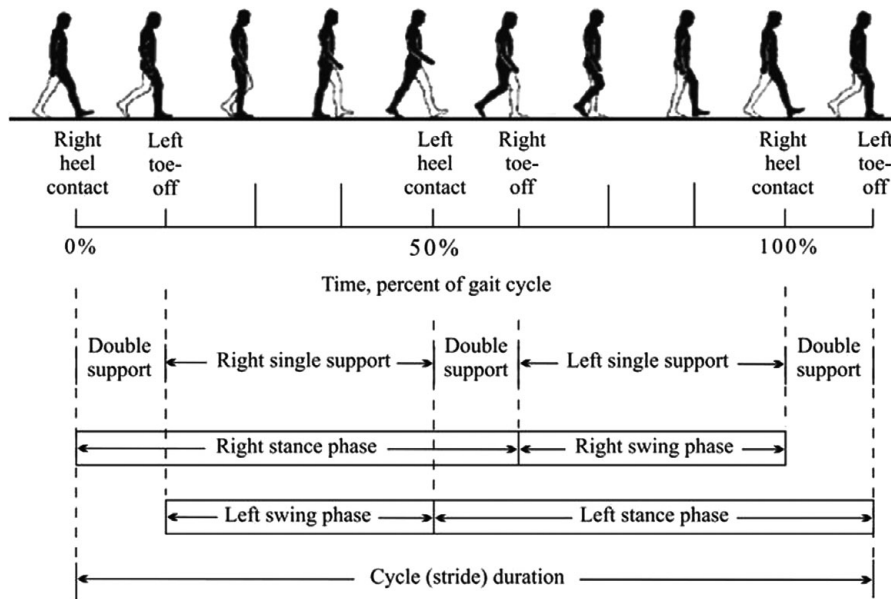
Fig. 3. Gait cycle (source: Inman *et al.*[45]).

starts by setting $\mathbf{f}_{n+1} = \mathbf{0}$ and $\mathbf{n}_{n+1} = \mathbf{0}$, where $n = 4$ is the number of links.

3. Gait Modeling

The gait cycle is the period of time between two identical events in the walking process.[2] A complete gait cycle is divided into two periods: stance phase and swing phase of the same leg. The left swing phase corresponds to the right SS phase and *vice versa*, where its duration constitutes approximately 40% of the gait cycle (Fig. 3). During an entire gait cycle the body performs two strides. The stride length is the distance covered by the same foot during a step. The SS is initiated with the trailing foot toe off and it lasts until its next ground contact (heel strike). The step length is the distance between the two feet at the beginning and at the end of a step. Let the SS phase duration be within the time interval $t \in [-T, T]$. When the average speed of the hips is given by v, then the step period $2T$ is defined as

$$T = \frac{sl}{2v}. \qquad (8)$$

For simplicity, we assume that the forward progression of the hips during the DS phase is infinitesimal.[37] In the sagittal plane, foot dimensions are foot height fh and foot length $a + b$ (Fig. 4). It has been shown that the swinging foot starts the SS with its heel raised, where the distance between the malleolus height and the ground $(mhi + fh)$ is around 0.17 m.[40] Moreover, during this phase, the stance foot is assumed to be completely fixed to the floor as described above, while the swinging foot motion should take into account the ground clearance. During the swinging, the trailing foot ankle tends to minimize dorsiflexion. Also, a certain foot elevation is necessary to deal with uneven nature of the floor. For these reasons, imposing the ground clearance has provided valid models in the literature.[6,8] In the current
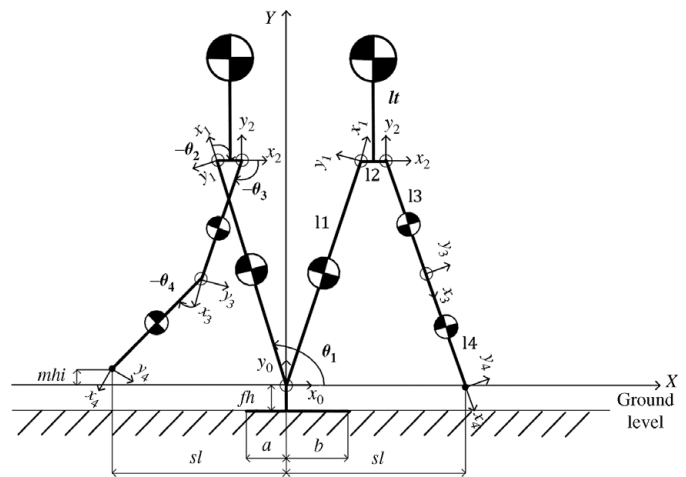
Fig. 4. Biped system model at instants $t = -T$ and $t = T$.

gait problem, this clearance is modeled by introducing the step height (sh) at the mid-stance.

4. Stability and Dynamic Gait Measure

In this paper, according to the assumptions described and justified previously, we consider the stability of the biped system during SS phase only, where the stance foot is in full contact with the ground while the swinging leg performs the stride. In the 2D sagittal plane, the stability region is constituted by the FSR, $x \in [-a, b]$ in the x-axis, and lateral stability is not considered here. Two commonly used ground reference points – GCOM and ZMP – are adopted as criteria in defining two types of gait, i.e., SW and DW.[26] When the ZMP resides within the FSR (Fig. 5), the gait is dynamically balanced,[19] in which case the ZMP coincides with the center of pressure,[20,46]

$$ZMP_x \in [-a, b]. \qquad (9)$$
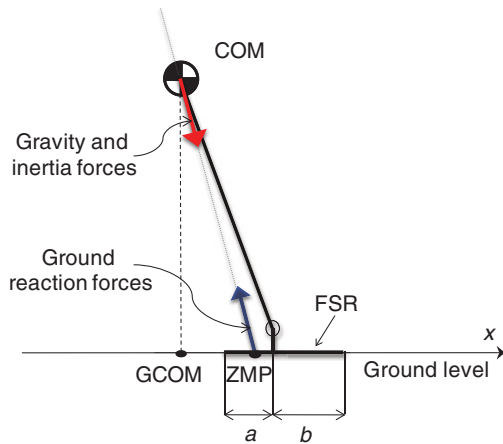
Fig. 5. (Colour online) ZMP and GCOM in the sagittal plane.

Theoretically, the ZMP criterion cannot be satisfied in limiting cases of edge or point contact between the foot and the ground.[19,20,24] In this theoretical event when the foot–ground contact occurs through edge or point, the center of pressure[46] that exists within the FSR or other inertia-based ground reference points that exist outside the FSR, such as the Foot-Rotation Indicator (FRI),[24] or the Fictitious Zero Moment Point (FZMP),[19] can be used for the stability criteria.[1] On the other hand, in reality, the foot is not ideally rigid but deformable, and any rotational inclination will transform the edge into a new surface.[19] Thus, physically the foot–ground contact always occurs through a finite (small or large) surface within which the ZMP exists, and therefore the ZMP criterion is always satisfied during robotic and human walking. This is also evident from many experimental observations of the ZMP[20] during both SS and DS phases of walking.

The position of the ZMP is calculated as follows:

$$\text{ZMP}_x = \frac{\sum m_i \bar{x}_i \left(\ddot{\bar{y}}_i + g \right) - \sum m_i \bar{y}_i \ddot{\bar{x}}_i + \sum \dot{L}_{z,i}}{\sum m_i \left(\ddot{\bar{y}}_i + g \right)}, \quad (10)$$

where $\bar{x}_i$, $\bar{y}_i$, $\ddot{\bar{x}}_i$, $\ddot{\bar{y}}_i$ are the positions and accelerations of the ith point mass m_i, represented in terms of joint angles θ_i. Here the time rate of change of angular momentum of each link about the z-axis ($\dot{L}_{z,i}$) is not included in the ZMP calculation due to the aforementioned point-mass assumption of the proposed biped model, in which the influence of $\dot{L}_{z,i}$ about each link's COM during walking has been shown to be negligible in the ZMP calculation,[6,41,42] particularly in the sagittal plane.

The stability criterion for SW refers to the GCOM position within the FSR at all time instants. Whenever the GCOM leaves the FSR, there is a presence of a statically unbalanced moment on the foot, which causes its rotation about a point on the FSR boundary.[24] The GCOM is calculated by considering only each link's mass, while inertia terms are not taken into account. Thus, GCOM position is obtained by removing the acceleration terms from the ZMP formula as follows (Fig. 5):

$$\text{GCOM}_x = \frac{\sum m_i \bar{x}_i g}{\sum m_i g}. \quad (11)$$

If a robot is stationary, it is shown that the center of pressure coincides with the GCOM.[24] Whether or not the GCOM should stay within the FSR depends on the gait. As described earlier, SW, which is usually performed by biped robots, requires that the GCOM exists within the FSR at all times, while the DW does not.

From definitions, the main difference between the ZMP and the GCOM is the effect of inertia (assuming gravity is the only externally applied force). Therefore, the distance between the ZMP and the GCOM at each time provides a measure of how dynamic is the current gait. To address the distance in x-direction over the time duration, the root mean square (RMS) of the distance between ZMP and GCOM is used, which can provide a measure of dynamicity:

$$\bar{d} = \sqrt{\frac{\int_{-T}^{T} \left[\text{ZMP}_x (t) - \text{GCOM}_x (t) \right]^2 dt}{2T}}. \quad (12)$$

Although the RMS distance quantifies certain degree of dynamicity by providing the effects of inertia, it lacks the information of relative stability due to dynamicity. To incorporate the relative stability into the measure of dynamicity, the RMS distance of a gait should be compared with that of a SW. In particular, the RMS distance for the limiting case of SW will provide a border between the SW and DW. In the case where the system is at rest, the ZMP and GCOM are equal, and the RMS distance becomes zero. It has been shown from our simulation experiments (and also in the results section) that, for SW of a 2D system, the ZMP position is almost at $x = 0$, and the GCOM follows a near-linear monotonic curve along the time from rear end to front end of the FSR. (The validity of these assumptions in 3D will be studied in future research.) Thus, given a foot size a and b, the RMS distance for the limiting static gait can be approximated as follows:

$$\bar{d}_{\lim} = \sqrt{\frac{\int_{-T}^{T} \left[\text{GCOM}_{\lim,x} (t) \right]^2 dt}{2T}} = \sqrt{\frac{a^2 - ab + b^2}{3}}, \quad (13)$$

where

$$\text{GCOM}_{\lim,x} (t) = \frac{a + b}{2T} (t + T) - a. \quad (14)$$

Finally, to represent the relative measure of dynamicity for a given gait motion and foot dimension, we define the dimensionless DGM as the ratio of the two RMS distances as follows:

$$\text{DGM} \left(\text{ZMP}_x, \text{GCOM}_x, a, b \right) = \frac{\bar{d}}{\bar{d}_{\lim}}$$

$$= \sqrt{\frac{\int_{-T}^{T} \left[\text{ZMP}_x (t) - \text{GCOM}_x (t) \right]^2 dt}{2T \left(a^2 - ab + b^2 \right) / 3}}. \quad (15)$$

Thus, the DGM is a functional of ZMP trajectory, GCOM trajectory, and foot dimension. Here it should be noted that the DGM, as a measure of the dynamicity of a gait, depends not only on the balance criteria such as ZMP and GCOM

but also on the stance foot dimension (i.e., FSR). Since the ZMP always exists and satisfies the criterion during robotic and human walking (as discussed above), the definition of DGM as a functional of ZMP trajectory is physically and mathematically valid. For a given walking motion and non-zero foot dimensions, the existence and uniqueness of the DGM can be easily checked from its definition.

From the above definition, it can be shown that the DGM is always positive (or zero) and is bounded from above as follows, as long as the stance foot maintains full contact with the ground during the gait:

$$0 \leq \text{DGM} \leq K, \tag{16}$$

where

$$K = \frac{\max\{d(\text{ZMP}_x, \text{GCOM}_x)\}}{\sqrt{(a^2 - ab + b^2)/3}} = \frac{\max\left\{\frac{1}{\sum_{i=1}^{4} m_i}\sum_{i=1}^{4}\left[m_i\left(\sum_{j=1}^{i-1} l_j + l_i c_i\right)\right] + a, \ \frac{1}{\sum_{i=1}^{4} m_i}\sum_{i=1}^{4}\left[m_i\left(\sum_{j=1}^{i-1} l_j + l_i c_i\right)\right] + b\right\}}{\sqrt{(a^2 - ab + b^2)/3}}, \tag{17}$$

where $d(\bullet, \bullet)$ is the distance between two points, and c_i is the fraction of the position of COM from the previous joint over the entire link length. It should be noted that the least upper bound, or supremum, K, can be calculated from link parameters (length, mass, COM of each link), stance foot dimension, and joint variable limits (here, for simplicity, full extension/flexion is assumed for each joint variable limit). In other words, when the stance foot is in full contact with the ground, the dynamicity of a biped walking is bounded from above by these system parameters, regardless of the maximum actuator torque capacity ($\tau_{i,\max}$) or muscle strength. Here K represents inherent potential of the dynamic nature of the gait. In other words, the K value indicates the maximum possible dynamicity of walking for a given biped system and foot dimension. Physically, larger foot dimension ($a + b$) should have smaller K. It should be noted that while DGM is dependent on the given gait parameters (e.g., speed and step length) as well as the biped system and foot dimension, K is independent of any gait parameters.

The DGM values can be interpreted according to several cases as follows:

- DGM = 0: The ZMP and GCOM are identical at all times. The motion of the system is stationary, or can be regarded as quasi-static.
- 0 < DGM < 1: The GCOM, as well as the ZMP, stays within the FSR during the gait. This indicates the SW. The smaller DGM values imply more statically stable than the larger ones.
- DGM = 1: The gait motion is marginally static, and its dynamicity is at the border between SW and DW.
- 1 < DGM ≤ K: The GCOM falls outside of the FSR at some times, while the ZMP stays within the FSR at all times. The larger DGM values imply more dynamic gait than the smaller ones. In other words, the existence of GCOM outside the FSR during longer duration or the larger distance between the ZMP and GCOM will result in larger DGM. According to the IPM analysis, larger distance between the GCOM and the ankle joint for a

given actuation capacity indicates higher tendency to fall at a time instant. Therefore, the DGM also indicates a time-global measure of instability during a gait.

In the Results section, the DGM will be calculated and used to evaluate the dynamicity and stability of walking for different sets of walking speeds, step lengths, and stance foot dimensions. It should be noted here that the proposed DGM formulation could be directly applied for the DS phase, in which case the FSR is the convex hull region formed by the two contacting feet.[19,26]

5. Optimality and Passive Gait Measure

From the viewpoint of minimum actuations, the idea of passivity in human walking is consistent with the optimality of the nature. The gait generation is formulated as an optimization problem, where the joint kinematic profiles and actuator torques are calculated under given constraints. Other physical quantities, such as the ZMP and GCOM trajectories, can be derived from the optimization solutions. The joint kinematics will be represented using the joint angle vector as follows:

$$\theta(t) = \begin{bmatrix} \theta_1(t) \ \theta_2(t) \ \theta_3(t) \ \theta_4(t) \end{bmatrix}^T. \tag{18}$$

A polynomial function is used to parameterize each joint angle profile. In order to guarantee the C^2 smoothness condition, i.e., continuous velocity and acceleration, the degree of polynomial should be at least three. From several numerical experiments using the proposed model for various cases, it has been found that higher order terms of the polynomials are negligible. Thus, to provide sufficient smoothness of the joint angle function, each joint is parameterized using the third order polynomial as follows:

$$\begin{aligned} \theta_1(t) &= \alpha_3 t^3 + \alpha_2 t^2 + \alpha_1 t + \alpha_0, \\ \theta_2(t) &= \beta_3 t^3 + \beta_2 t^2 + \beta_1 t + \beta_0, \\ \theta_3(t) &= \gamma_3 t^3 + \gamma_2 t^2 + \gamma_1 t + \gamma_0, \\ \theta_4(t) &= \delta_3 t^3 + \delta_2 t^2 + \delta_1 t + \delta_0, \end{aligned} \tag{19}$$

where the coefficients $\alpha_i, \ \beta_i, \ \gamma_i, \ \delta_i \ (i = 1, 2, 3, 4)$ are the optimization variables.

To generate the walking motion that demonstrates (partial) passivity, the actuator torques should be included in the cost function. As discussed earlier, various ways of implementing the actuator torques into the cost function have been developed in the literature; this is also consistent with previous studies suggesting that, for a given progression velocity, human chooses a gait that minimizes the energy consumption.[1,2,28−36] The proposed cost function is a weighted squared norm of actuator torque vector function

for the time interval $[-T, T]$, as follows:

$$J = \int_{-T}^{T} \left(w_1 \tau_1^2 + w_2 \tau_2^2 + w_3 \tau_3^2 + w_4 \tau_4^2 \right) dt, \qquad (20)$$

where τ_i is the actuator torque at the ith joint, and w_i is the corresponding weight function. The quadratic expression of the actuator torques ensures that opposite signs are not cancelled with each other in the cost function, and that there exists a continuous first derivative for gradient-based optimization. By minimizing this cost function, the walking motion will be generated with as much passivity as possible under the given constraints and gait parameters.

In general, the values of the weight function w_i depend on the criteria of the problem. Here we propose the physiologically inspired weight functions such that the cost function has characteristics that mimic the human energetics, in particular the heat expenditure, which is known as directly proportional to the muscle force and inversely proportional to the maximum muscle strength.[47–51] As a consequence, the relative passivity weight is defined as the weight function value at each joint that is inversely proportional to the squared maximum actuation capacity as follows:

$$w_i = \frac{k}{\tau_{i,\max}^2}, \quad \sum_{i=1}^{4} w_i = 1, \qquad (21)$$

where k is a proportionality constant with dimension of $[1/s]$, such that the functional is dimensionless. For numerically sound performance of the optimization algorithm, a property similar to the partition of unity is imposed to the passivity weights. From the data available in the literature[38,40] for the ankle, knee, and hip joints, the following relationship can be assumed during the SS phase:

$$\tau_{2,\max} \simeq \tau_{3,\max} \simeq \tau_{4,\max} \simeq 2\tau_{1,\max}. \qquad (22)$$

Therefore, the passivity weight vector is calculated as follows:

$$\mathbf{w} = [0.571, \ 0.143, \ 0.143, \ 0.143]. \qquad (23)$$

It can be seen from the proposed cost function and passivity weights that human gait of minimum energy consumption (thus minimum weighted actuator torques) implies that human tends to use the stronger joints (knee and hips) rather than the weaker one (ankle). This means that the actuator torques are distributed in such a way that the larger torques are exerted at the knee and hip joints and smaller torques at the ankle joint. From multi-objective optimization viewpoint, the proposed passivity weights naturally enforce that the stance ankle torque (with larger weight) is more minimized than other joints (with smaller weights), thus controlling the relative passivity of the joints. The reinforced minimization of the ankle joint torque by the proposed passivity weights is also consistent with the concept of IPM (where the unactuated hinge corresponds to the human ankle joint) and

many other models in the literature that used the minimum ankle torque to generate gait motions.[28–30]

Based on the proposed biped system and gait model, initial/final conditions and gait constraints are imposed to the variables as follows:

- Initial and final position along x- and y-axes of the swinging ankle is calculated by the step length chosen for the gait:

$$x_4(-T) = -sl; \quad x_4(T) = sl; \quad y_4(-T) = mhi;$$
$$y_4(T) = 0. \qquad (24)$$

- Ground penetration should be avoided. In particular, the step height is imposed (within a tolerance ε) during the mid-stance to ensure ground clearance, which is a common constraint used in the literature[6,8]:

$$y_4(t_i) \geq 0; \ y_4(0) = sh \pm \varepsilon. \qquad (25)$$

- The knee joint angle should be bounded within its range of motion to avoid hyperextension during the swinging motion. Also, according to Saunders *et al.*,[52] the swinging leg is almost fully extended at the time of heel strike:

$$\theta_4(t_i) \leq 0; \quad \theta_4(T) = 0. \qquad (26)$$

- The swinging hip joint angle should be bounded within its range of motion. In addition, the hip angle is further bounded as it initiates the swinging phase from toe-off:

$$\theta_3(t_i) \leq 0; \quad \theta_3(-T) \leq -\frac{\pi}{2}. \qquad (27)$$

- The torso maintains almost vertical position during SS (Fig. 4) due to small oscillations in normal human walking.[52] This constrains link 2 to be always horizontal during SS, which also ensures right–left symmetry assumption for simplicity:

$$\theta_1(t_i) = -\theta_2(t_i). \qquad (28)$$

- The ZMP-based stability is also considered. In this case, rather than imposing the constraints directly into the optimization algorithm for motion generation, the ZMP values are monitored throughout the motion to ensure that the ZMPs always exist within the FSR boundary.

The stable walking (without falling) is ensured if all the constraints are satisfied. The existence of the optimal solution indicates that the physically consistent gait motion is generated according to the initial and final foot positions while maintaining the ZMP constraints under given actuation capacities. This analysis applies to walking motions with various dynamicity levels, including those for DGM > 1. If the gait with given parameters results in instability (due to either ZMP violation or insufficient actuation capacities), then the optimization algorithm will result in infeasibility and the required walking motion cannot be generated.

All constraints are functions of joint angles at each time step t_i, and thus they are also the functions of optimization variables α_i, β_i, γ_i, δ_i. The cost function and the constraints

are implemented into the optimization algorithm by the "NMinimize" command in Mathematica©, which uses merit-based choice between the Nelder–Mead algorithm and the differential evolution methods.

Since no walking machine or bio-mechanism can be fully passive (except for walking down a slope), the relative passivity, rather than the absolute passivity, should be considered. As described earlier, based on the IPM analogy and the minimization of physiologically inspired passivity weights, the degree of passivity in biped walking is associated with the actuator torque exerted at the stance ankle. In normal DW, the link dynamics and the gravity contribute to the gait motion, allowing less actuator torques at the ankle joint; while the effect of inertia is relatively small in SW, which requires the larger ankle torque.

In order to quantify the contribution of τ_1 over the time duration, we use the RMS representation as follows:

$$\bar{\tau}_1 = \sqrt{\frac{\int_{-T}^{T} \tau_1(t)^2\, dt}{2T}}. \tag{29}$$

However, although the RMS ankle torque provides absolute magnitude, its relative contribution to the gait depends on the dynamics of the whole biped system. In other words, applying the same ankle torque for the gait of a small/light system and a large/heavy system will demonstrate different levels of passivity. In order to quantify the relative passivity, the dynamics of the whole biped system should be considered. Since the dynamic effects (mass, moments/products of inertia, gravity, external loads, and momentum) are incorporated into the actuator torques at all joints through the equations of motion, the relative passivity can be described as the ratio between the RMS of the ankle torque ($\bar{\tau}_1$) and the RMS of the total actuation ($\bar{\tau}_{\text{tot}}$). Therefore, the dimensionless PGM is defined as follows:

$$\begin{aligned}
\text{PGM}(\tau_1, \tau_2, \tau_3, \tau_4) &= 1 - \frac{\bar{\tau}_1}{\bar{\tau}_{\text{tot}}} \\
&= 1 - \sqrt{\frac{\int_{-T}^{T} \tau_1^2\, dt}{\int_{-T}^{T} \left(\tau_1^2 + \tau_2^2 + \tau_3^2 + \tau_4^2\right) dt}},
\end{aligned} \tag{30}$$

where

$$\bar{\tau}_{\text{tot}} = \sqrt{\frac{\int_{-T}^{T} \left(\tau_1(t)^2 + \tau_2(t)^2 + \tau_3(t)^2 + \tau_4(t)^2\right) dt}{2T}}. \tag{31}$$

The PGM quantifies the relative contribution of τ_1 with respect to the total actuation of the biped system. It represents the relative passivity for the given gait parameters and biped system model, which can be shown to be bounded as follows:

$$0 \leq PGM \leq 1, \tag{32}$$

where
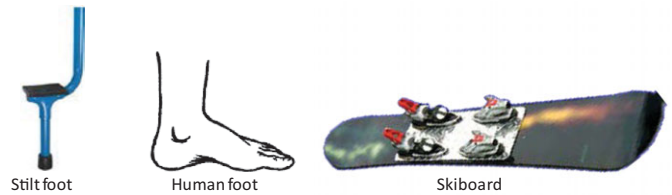
Fig. 6. (Colour online) Different foot dimensions.

- PGM = 0: only the stance ankle joint is actively controlled, while all other joint actuator torques are zero at all times;
- 0 < PGM < 1: the stance ankle joint as well as some or all other joints are actuated. Larger PGM values indicate that the gait of the system is rather passive, while smaller values indicate that the ankle joint is more actively controlled;
- PGM = 1: the stance ankle actuator torque is zero at all times. This is the case of fully passive walking with respect to the ankle joint, in which the stance leg acts like an ideal IPM with unactuated hinge.

Since the gait constraints cannot be satisfied with a completely unactuated system, a unique PGM value exists for a given walking motion and foot dimension. In the Results section, the PGM will be calculated and used to evaluate the optimality and passivity of walking for different sets of walking speeds and step lengths.

6. Results and Discussion

To demonstrate the PGM and DGM, the gait motions are generated for human-like walking (which is relatively passive and dynamic) and robotic walking (which is actively controlled and mainly statically stable) using the proposed optimal control scheme and physiologically inspired weighted torques. Here, for simplicity, we differentiate the human-like walking and robotic walking by different sets of walking speeds and step lengths, although practically they are characterized by many additional features, such as model structures and control methods. The biped system model parameters, such as mass distribution and link lengths, and dynamic parameters are assigned based on a human anthropometry of total body mass of 75 kg and height of 1.8 m (Table I).[38]

The Mathematica© program is used for computational implementation of the proposed formulations. For each example, the kinematics, actuation, ZMP, and GCOM are calculated. The proposed RMS distance, RMS torques, DGM, and PGM are also calculated and analyzed. In particular, to demonstrate the dynamic nature of biped gait as associated with the stability and its dependence on the FSR, the DGM is evaluated for three cases with distinct foot dimensions – normal human foot: $(a, b) = (10, 20)$, total length = 30 cm; stilt foot: $(a, b) = (5, 5)$, total length = 10 cm; and skiboard: $(a, b) = (35, 35)$, total length = 70 cm (Fig. 6). Selected result data and some qualitative interpretations are discussed.

6.1. Human-like walking
The walking speed and step length are given in Table II, which correspond to the self-selected parameters of normal walking performed by the human model compatible with the proposed

Table II. Parameters for human-like walking.

Parameters	Value
Velocity (v [m/s])	1.53
Malleolus height (mhi [m])	0.07
Step length (sl [m])	0.5
Step height (sh [m])	0.1
Foot height (fh [m])	0.1

Table III. Parameters for robotic walking.

Parameters	Value
Velocity (v [m/s])	0.3
Malleolus height (mhi [m])	0.07
Step length (sl [m])	0.35
Step height (sh [m])	0.1
Foot height (fh [m])	0.1
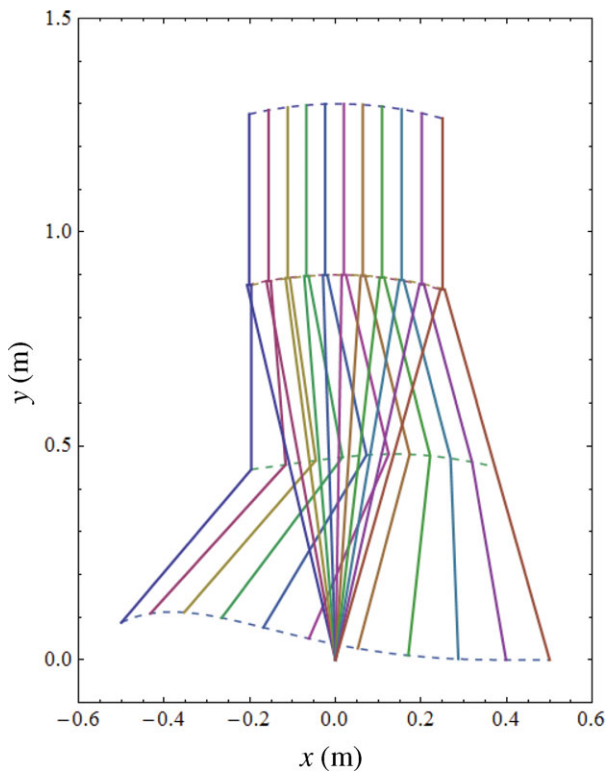
Fig. 7. (Colour online) Generated human-like walking motion.

biped system. Then the joint profiles (motion), required actuator torques, ZMP trajectory, and GCOM trajectory are calculated as the outputs of the proposed optimization algorithm (Figs. 7, 8, 15, and 16).

Also, the kinematic profiles of the torso (m_2) and the swinging ankle (foot) are plotted as functions of time in forward and vertical directions (Figs. 9 and 10). The snapshots of the result (Fig. 7) show a near-natural human-like walking motion. For the purpose of this research, where the proof-of-concept demonstrations focus on the difference in DGM and PGM for human and robotic gait motions characterized by different sets of walking speeds and step lengths, rather than on generating a completely realistic human walking motion, partial validation of the results is discussed here, while more rigorous validation is proposed as future work later in this section. Two aspects can be considered for partial validation of the generated human-like walking motion. First, since some of the constraints imposed on the system model and the optimization algorithm are based on the realistic human gait data, the associated segments naturally ensure the generation of realistic human walking motion. These include the constant stance knee angle in Link 1,[30,38] the full extension of the swinging

knee at heel strike,[52] the horizontal pelvic global angle of Link 2 in the sagittal plane,[52] and the walking speed and step length. Second, the qualitative comparison of the results in terms of both magnitudes and patterns is used as a validation method, which is a widely accepted approach in the literature.[38,53] The patterns of the joint trajectories (Fig. 8 (left)), actuator torques (Fig. 15), torso trajectory (Fig. 9), and swinging foot trajectory (Fig. 10) show matching trends with experimentally measured data for real human subjects available in the literature.[40,53] In addition, the joint angle ranges and magnitudes (Fig. 8 (left)) for the stance ankle dorsiflexion, stance hip extension, swinging hip flexion, and swinging knee flexion/extension, as part of the standard determinants,[52] show very good similarity with the experimental data.[53] These provide sufficient partial validation of the generated human-like walking motion for the given purpose of this research.

6.2. Robotic walking
To demonstrate the proposed DGM and PGM with a counter-example to the human-like walking, a mainly statically stable robotic walking motion is generated with lower speed and smaller step length. The gait parameters v and sl are chosen based on the typical ranges of speed and step length of humanoid robots available in the literature[6,8,22,25] (0.15–0.4 m/s and 0.2–0.5 m). The specific gait parameters used in the current problem are listed in Table III.

Again, the joint profiles, required actuator torques, ZMP, GCOM, and kinematic profiles of the torso and the swinging foot are calculated as the outputs of the proposed algorithm (Figs. 11–16). Compared with the results of the human-like walking, the notable difference is in the ankle actuator torque. The ankle actuator torque for the robotic walking is much larger than that of human-like walking, indicating that the statically stable walking requires more active control at the ankle joint. This large ankle torque is also in line with the less dynamic nature of the SW, where the contribution of the gravity force to the ankle moment is small due to the short distance between the ankle and the GCOM. Further analysis will be discussed along with the calculated PGM and DGM values in the next section.

6.3. PGM and DGM: human vs. robotic gait
Based on the calculated results for the walking motion (Table IV), the problems of "optimality and passivity" and "stability and dynamicity" are analyzed.

6.3.1. Optimality and passivity. The walking motion of each case is obtained through the optimality of the passivity-weighted actuator torques under the given gait parameters
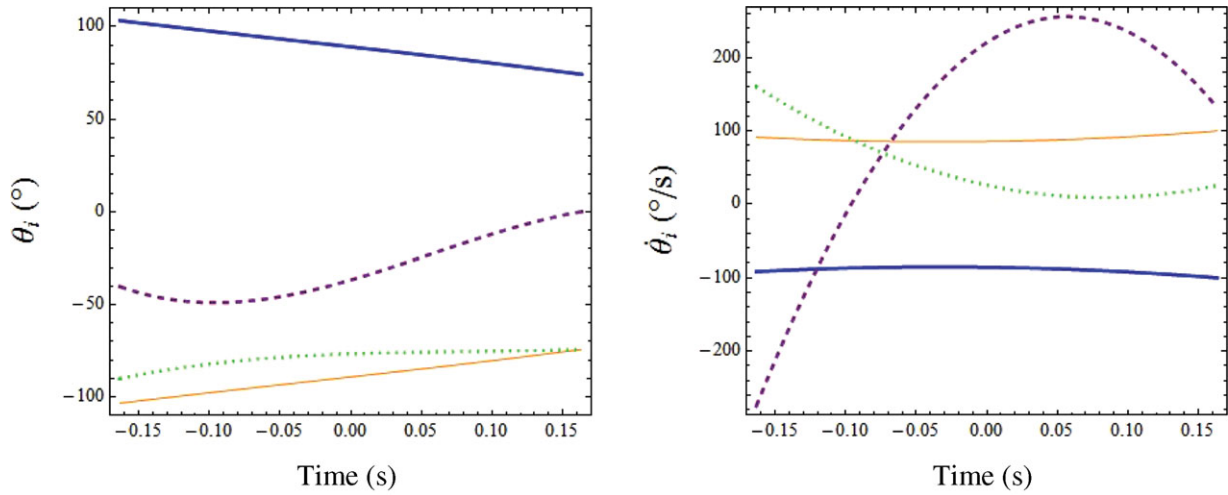
Fig. 8. (Colour online) Joint angles (left) and velocities (right) at the stance ankle (thick), stance hip (solid), swinging hip (dotted), and swinging knee (dashed) for human-like walking.
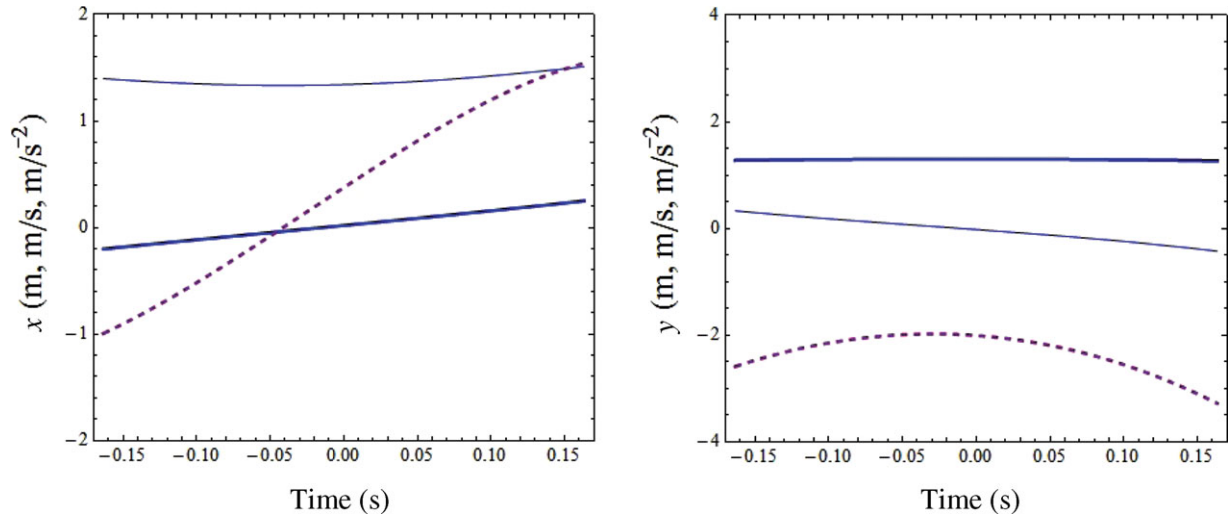
Fig. 9. (Colour online) Torso point mass displacement (thick), velocity (solid), and acceleration (dashed) for human-like walking in forward x-direction (left) and vertical y-direction (right).
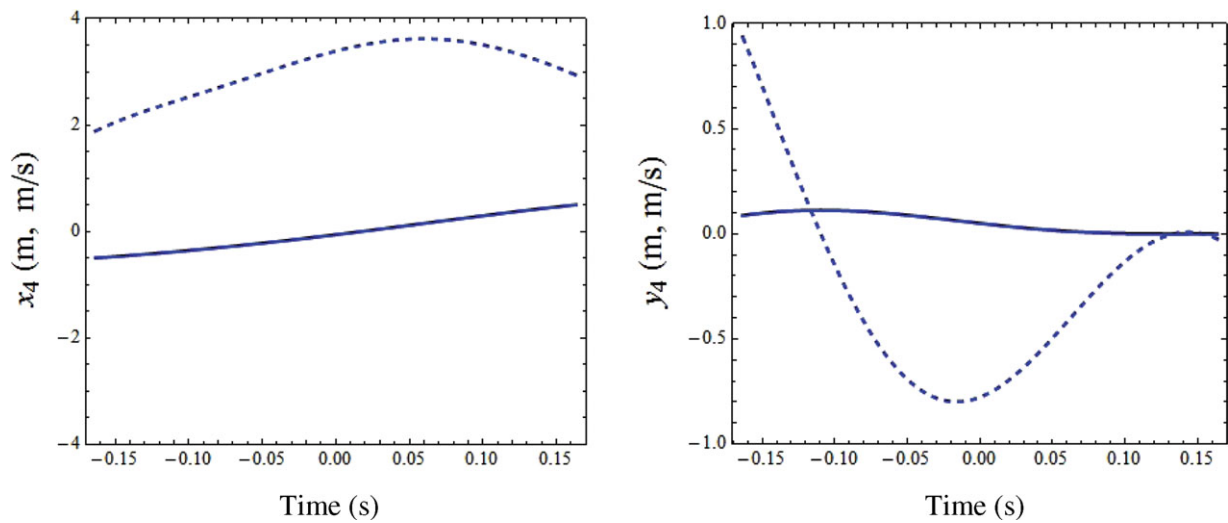
Fig. 10. (Colour online) Swinging ankle displacement (solid) and velocity (dashed) for human-like walking in forward x-direction (left) and vertical y-direction (right).

Table IV. Cost function value, PGM, RMS distance, upper bound *K*, and DGM.

	Human-like	Robotic	
Cost function value	7.162	41.644	
PGM	0.712	0.2	
RMS distance $\bar{d}$ (m)	0.139	0.068	
DGM stilt foot (10 [cm])	4.388	2.150	$K = 33.08$
DGM human foot (30 [cm])	1.294	0.634	$K = 11.05$
DGM skiboard (70 [cm])	0.627	0.307	$K = 6.21$
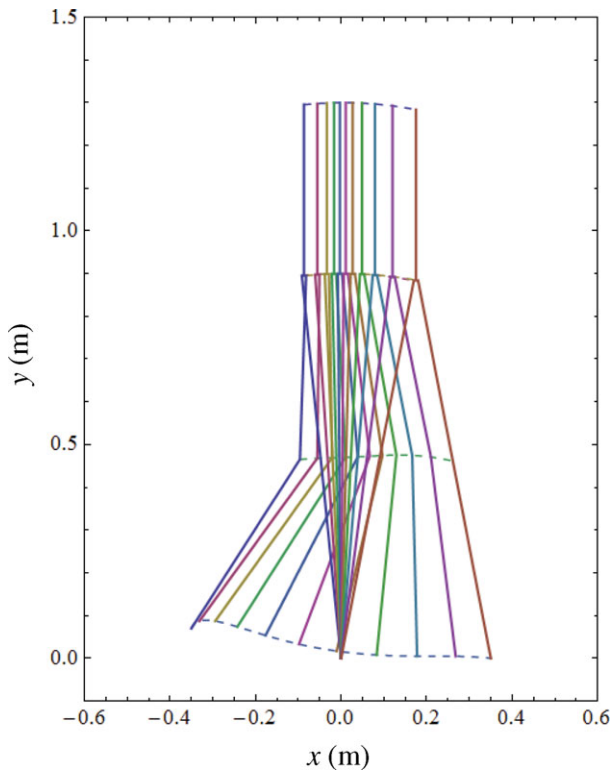
Fig. 11. (Colour online) Generated robotic walking motion.

and constraints. The required joint actuator torques for both gaits are consistent with the generated motion (Fig. 15). Although the patterns for both gaits are similar, the human-like walking requires less actuator torques overall. In particular, the ankle actuator torque for the human-like walking is much less than that of the robotic walking, indicating that the human gait is more passive than the robotic gait, from the perspective of the IPM. The natural selection of the passivity weights in the cost function based on the physiologic energy consumption leads to the gait motion that is generated according to the reinforced minimization of the ankle torque. Therefore, the proposed passivity weights, along with the resulting actuator torques for the human-like walking, support the IPM analogy.

The difference in the actuation is also evident from the resulting cost function value, which is much smaller for the human-like walking (7.162) than for the robotic walking (41.644). Since the proposed cost function is formulated on the analogy of the physiologic heat dissipation, it represents a measure of actuation effort or a dimensionless approximation of energy consumption. Therefore, these cost function values also represent a dimensionless measure of the cost of transport for each walking motion, which is defined as the energy consumption per unit weight and unit distance travelled.[54–56] The comparison of the cost function values also suggests that the natural human walking with self-selected speed and step length demonstrates less total actuation (energy consumption) compared with the gait with lower speed and smaller step length. This result partially verifies another optimality of the human-like walking in terms of speed.[2,31]

Note that the cost function value indicates the overall optimality and a rough measure of total passivity, but it cannot be used to indicate the relative passivity of the ankle joint in general. The resulting PGM values for both human-like walking (0.712) and robotic walking (0.2) provide the quantified measures of the relative passivity, where large PGM indicates higher passivity and *vice versa*. While the cost of transport has a positive relationship with the physiology-inspired cost function, it is not necessarily coupled with
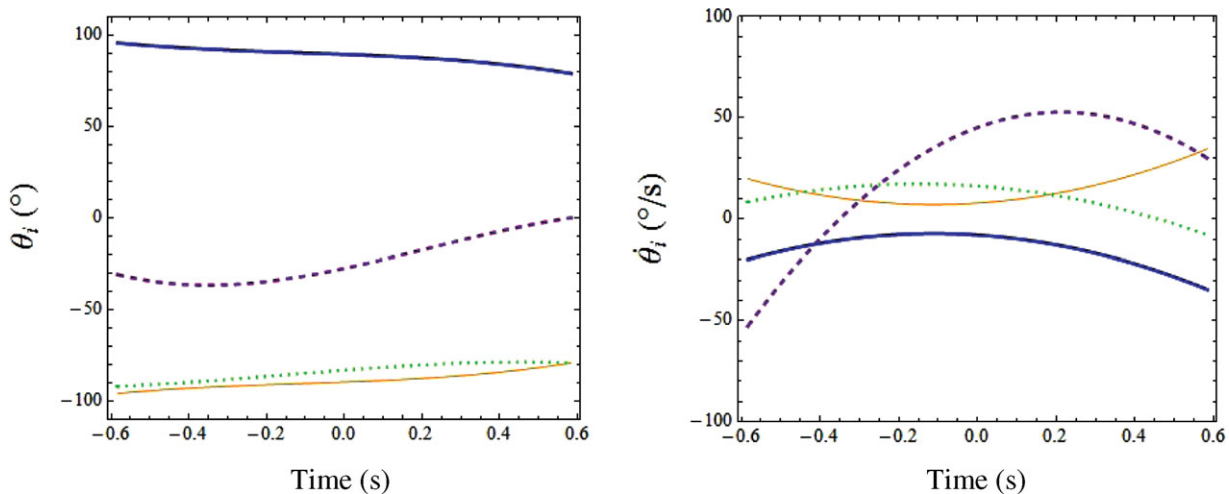
Fig. 12. (Colour online) Joint angles (left) and velocities (right) at the stance ankle (thick), stance hip (solid), swinging hip (dotted), and swinging knee (dashed) for robotic walking.
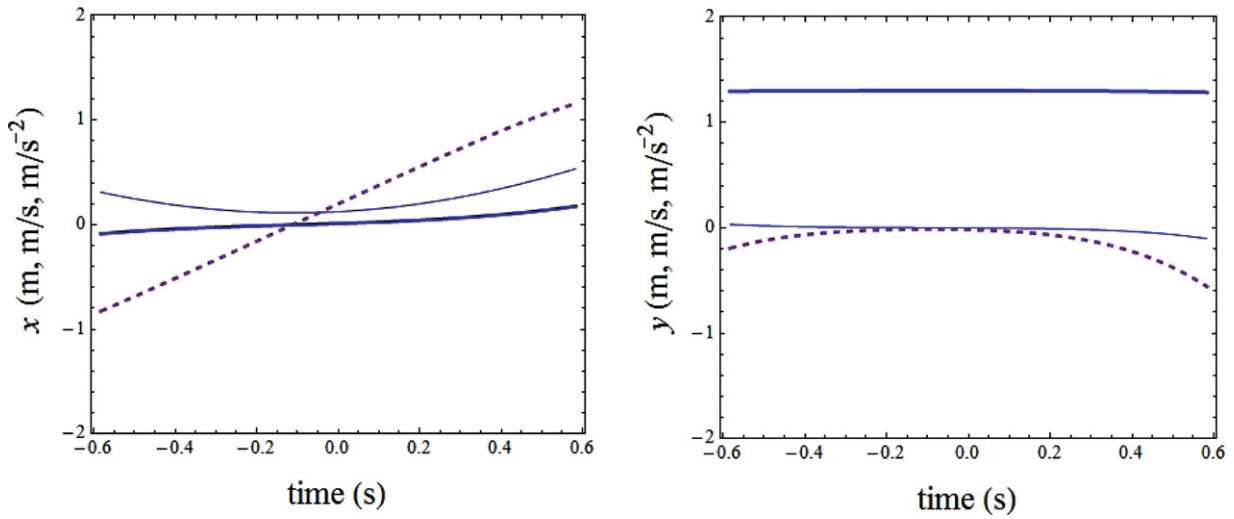
Fig. 13. (Colour online) Torso point mass displacement (thick), velocity (solid), and acceleration (dashed) for robotic walking in forward *x*-direction (left) and vertical *y*-direction (right).
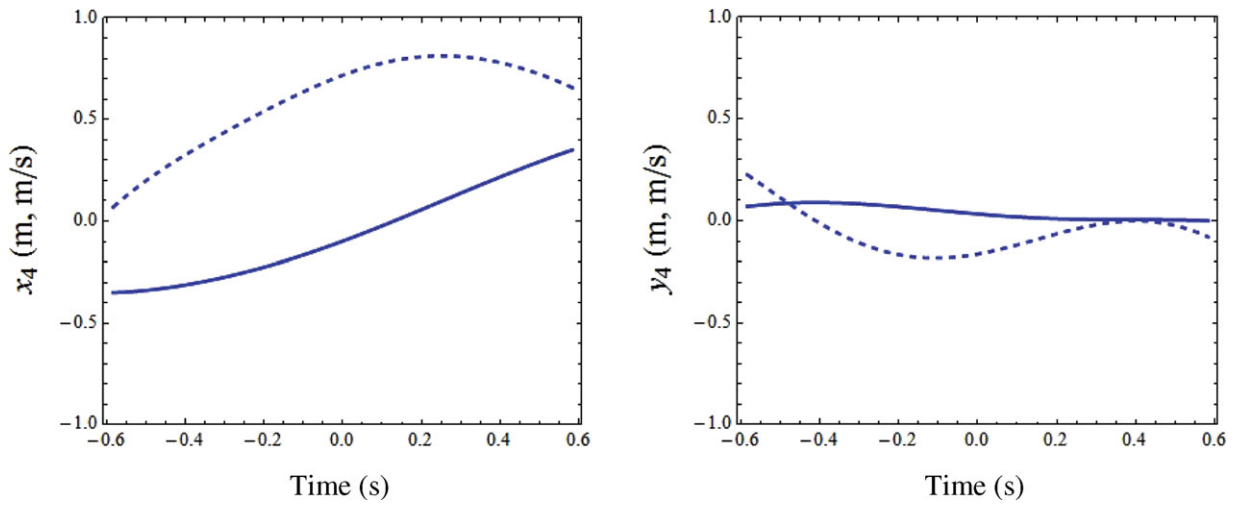
Fig. 14. (Colour online) Swinging ankle displacement (solid) and velocity (dashed) for robotic walking in forward *x*-direction (left) and vertical *y*-direction (right).
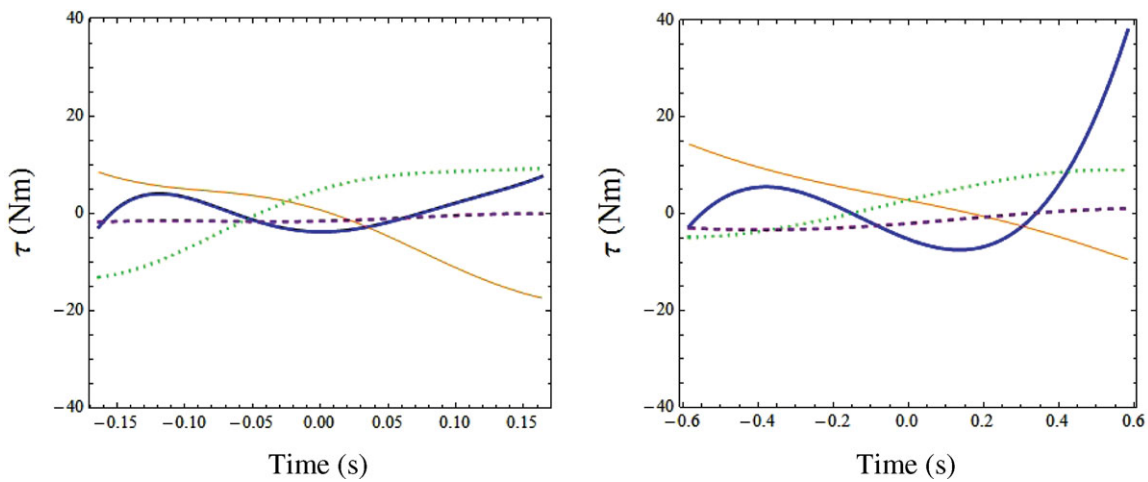
Fig. 15. (Colour online) Actuator torque at stance ankle (thick), stance hip (solid), swinging hip (dotted), and swinging knee (dashed) for human-like (left) and robotic (right) walking.
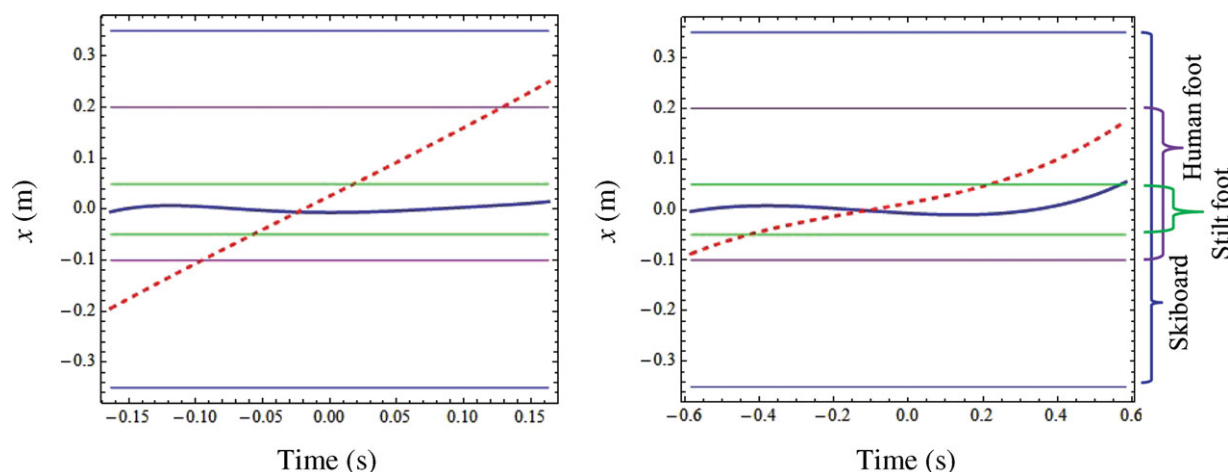
Fig. 16. (Colour online) ZMP (solid) vs. GCOM (dashed) for human-like (left) and robotic (right) walking.

PGM for general gait motions. This is because if the stance ankle actuation is small while the other joint actuations are large (due to additional task requirements or environmental constraints), the walking is relatively passive, but the cost function and the cost of transport maintain large values; similar arguments can be made for the opposite case. However, for naturally coordinated walking motions – such as normal human walking – to which all body segments are dedicated, the whole body actuations are minimal and are associated with the stance ankle actuation; in these cases, the PGM is also consistent with the cost of transport. Since the PGM represents relative contribution of the ankle torque compared with the total actuations, the results suggest and verify that normal human walking is more passive (at the ankle) than robotic walking.

6.3.2. Stability and dynamicity. The transition of the system's COM in the forward direction is consistent with the calculated GCOM trajectories. Although the ZMP trajectories for both gaits are similar in term of the magnitude and the shape, the GCOM trajectories show significant difference (Fig. 16). This is also evident from the calculated RMS distances. The similar ZMP trajectories, which are located close to the ankle joint ($x = 0$), are due to the compensation of large and small inertia for large and small GCOM magnitude respectively; this feature is also consistent with the experimentally measured data for human subjects[20] and robotic control methods,[6,8,22] which serves as partial validation of our simulated results.

For all foot dimensions (stilt foot, human foot, and skiboard) and for both gaits, the ZMP stays within the FSR; this indicates that the generated motions are physically feasible. (If the ZMP tends to demonstrate large magnitude, then the ZMP constraint should be additionally implemented into the optimization algorithm to ensure physical consistency.) The GCOM of the human-like walking is maintained within the skiboard FSR, while it falls outside the FSR during certain period for stilt and the human foot. On the other hand, the GCOMs of robotic walking with both skiboard and the human foot are maintained within the FSR. The GCOM falls outside of only the stilt foot FSR for robotic walking. The results indicate that providing a larger support

to the stance foot, for example with a skiboard, ensures the GCOM to stay within the FSR (thus statically stable) during the entire SS for both human-like walking and robotic walking. This is seen from the real-world experience where a human with skiboard on does not fall within the sagittal plane. On the other hand, a smaller FSR (e.g., stilt foot) makes the GCOM fall outside the foot/ground contact region for most of the time, indicating that the dynamic effect is dominant for both human-like walking and robotic walking. The average human foot shows DW for human-like walking parameters, and SW for robotic walking parameters.

From above the physically valid analysis can be quantified more rigorously by the calculated DGM for each case, where the DGM of 1 is the threshold between SW and DW. A DGM greater than 1 indicates DW, while less than 1 indicates SW. The calculated K values – the upper bounds of DGMs – indicate maximum inherent potentials of the dynamicity of walking for each foot dimension. It can be seen that larger foot dimensions result in smaller K values (stilt $K = 33.08$, human foot $K = 11.05$, and skiboard $K = 6.21$), which is consistent with its physical interpretation. Overall, the DGMs for human-like walking are larger than those for the robotic walking. The larger the DGM, the more dynamic the walking. For example, the human gait with stilt foot is more dynamic than the robotic gait with the stilt foot and the human gait with the human foot. Similarly, as the DGM approaches to zero, the gait becomes more statically stable. The robotic gait with skiboard is more statically stable than the robotic gait with the human foot and the human gait with skiboard. The DGM values for the human foot support base verifies the DW (DGM > 1) for human-like walking with average speed, and SW (DGM < 1) for robotic walking – a result that is consistent with the experiments in the literature.[25] The results can also be used to predict the characteristics of the DGM in more detailed human gait realization. The increased DGMs for decreased foot dimensions indicate that if the stance foot contact is further segmented to include the heel and toe contacts that have smaller contact surfaces, the overall DGM will be larger than the above value. This indicates that the above DGM result for full foot contact can be considered as the minimum value for the given gait, which represents a valuable quantitative measure that can be used

to compare different gait parameters and foot dimensions. In addition, the increased DGM for human gait with full foot and toe contacts will demonstrate a valid and even convincing dynamic nature of normal human walking as compared with the robotic walking. Overall, it can be seen that the DGM provides a single reliable measure for the dynamicity level of the given gait parameters and foot dimension.

As discussed above, the resulting small ankle torque for human-like walking is also in line with the more dynamic nature of human gait. In fact, the dynamicity and the passivity of biped walking are related to each other, particularly for normal human walking. This is because usually the passivity is achieved by the contribution of the gravity force and momentum. Before the heel strike of normal human walking, the moment about the ankle joint due to the gravity force increases as the GCOM moves farther away from the ankle location. Then the acquired momentum leads to a reduced required ankle actuation after the toe-off of the swinging leg. Since the ZMP is located close to the ankle joint in human-like walking (under the current simple model), the passivity will increase as the dynamicity increases. Although the dynamicity and the passivity are usually coupled in normal human walking, it is not necessarily true for general gait motions such as unnatural human walking and robotic walking. In general, the DGM and PGM are independent and both should be evaluated independently. As evident from the proposed mathematical formulation, the variables used in each measure are not necessarily dependent on each other. In other words, the GCOM and ZMP are determined by not only the actuator torques but also the initial and boundary conditions of the system and any applied external loads (if exists) other than the gravity. Also, depending on the foot dimension, step length, and walking speed, the coupling between the DGM and PGM can diminish. For example, walking with small ankle actuation for small step length and large foot dimension will result in high passivity but low dynamicity. On the other hand, it is also possible to exert large ankle actuation for unnatural walking with large step length and small foot dimension, which will result in low passivity and high dynamicity. It can be stated that, particularly for unnatural human (e.g., due to injury or heavy backpack) or robotic walking, the correlations between the PGM and DGM are weaker than those for normal human walking.

6.4. Future work on experimental demonstration and validation using more detailed models

The research in this paper was focused on initial concepts, mathematical formulations, physical analyses, and computer simulations of the proposed DGM and PGM, based on the supporting scientific motivations. The proof-of-concepts results demonstrated the validity and reliability of the proposed initial concepts in the 2D sagittal plane, and promise that the PGM and DGM concepts can be well applied to more detailed models. On the other hand, an extended future research, including the experiments for actual walking machines and human subjects, is required to demonstrate the broad and general applicability of the concepts and to validate their proof-of-practice in realistic gait. In addition, the experimental analysis can also provide

feedback for refinement and improvement of the DGM and PGM formulations.

However, experimental measurements of the required parameters involve several major challenges. The ZMP, GCOM (both for DGM calculation), and the inverse-dynamics-based joint actuator torques (for PGM calculation) require the measurements of motion kinematics, ground reaction forces and moments, and body segment inertial parameters. While the measurements of motion kinematics and ground reaction forces/moments are relatively straightforward by using motion capture camera systems and force plates, respectively, the estimation of inertial parameters of the complex 3D high degrees of freedom biped system (real robots and humans) requires another in-depth research. Although the conventional linear methods of parameter estimation have been extended to human/humanoid systems[57], a nonlinear approach has to be established for more accurate identification of inertial parameters of multi-segmental systems. In addition, more detailed gait realization will require more detailed and extensive models of the foot with additional degrees of freedom at the toe-ball joint and the contact dynamics for the transition from full foot to toe contact, which will result in the ankle position change and time-varying foot contact surface during SS; these problems are not completely resolved in the current gait literature. Therefore, the development of this framework, along with the effort required for experimental design and set up, poses a new set of extensive research problems, which will be addressed in our future work.

7. Conclusion

Normal human walking is usually characterized as passive and dynamic. Nevertheless, human walking is neither fully passive nor constantly dynamic, and the quantification of the level of passivity and dynamicity has not been rigorously addressed in the literature. In this paper, we proposed initial formulations of two quantitative measures – PGM and DGM – of biped walking. The passivity weight functions were introduced and incorporated in the actuation cost to generate walking motions. Using a simple planar biped model, two different walking motions – human-like and robotic – were generated from given walking speeds and step lengths. The human-like walking results showed better optimality and more passivity than the robotic walking. The relative passivity of each gait was quantified by introducing the PGM, where the PGM value for the human-like walking was greater than that of the robotic walking; this result validated the relatively passive nature of human walking. While the stability of the generated gait motions was characterized by the ZMP and GCOM, the dynamicity was quantified as the proposed DGM. In general, the DGMs for human-like walking were greater than those for robotic walking, verifying the dynamic nature of human gait. The resulting DGMs also demonstrated their dependence on the stance foot dimension as well as the walking motion. For a given walking motion, smaller stance foot dimension resulted in increased dynamicity and *vice versa*. Thus, the proposed PGM and DGM provide a single measure of passivity and dynamicity, respectively, of a given biped walking motion

in the sagittal plane. The extension and application of the proposed concepts to 3D walking motion will be studied as future research, where a statistically significant number of gait parameter sets will be used to demonstrate these measures. In addition, more accurate data on the mass and inertia parameters will improve the model with more realistic results. Also, future experimental measurements of PGM and DGM with many human subjects will provide normal ranges for these values. The proposed results will benefit the human gait studies and the development of walking robots and prosthetic mechanisms.

References

1. Y. Xiang, J. S. Arora and K. Abdel-Malek, "Physics-based modeling and simulation of human walking: A review of optimization-based and other approaches," *Struct. Multidiscip. Optim.* **42**, 1–23 (2010).
2. V. Racic, A. Pavic and J. M. W. Brownjohn, "Experimental identification and analytical modelling of human walking forces: Literature review," *J. Sound Vib.* **326**, 1–49 (2009).
3. A. D. Kuo, J. M. Donelan and A. Ruina, "Energetic consequences of walking like an inverted pendulum: Step-to-Step transitions," *Exercise Sport Sci. Rev.*, **33**(2), 88–97 (2005).
4. A. D. Kuo, "The six determinant of gait and the inverted pendulum analogy: A dynamic walking perspective," *Hum. Mov. Sci.* **26**, 617–656 (2007).
5. C. L. Vaughan, "Theories of bipedal walking: An odyssey," *J. Biomech.* **36**, 513–523 (2003).
6. A. Albert and W. Gerth, "Analytic path planning algorithms for bipedal robots without a trunk," *J. Intell. Robot. Syst.* **36**, 109–127 (2003).
7. J. H. Park and K. D. Kim, "Biped Robot Walking Using Gravity-Compensated Inverted Pendulum Mode and Computed Torque Control," **In**: *Proceedings of the IEEE International Conference on Robotics and Automation*, Leuven, Belgium (May 1998), vol. 4, pp. 3528–3533.
8. T. Ha and C.-H. Choi, "An effective trajectory generation method for bipedal walking," *Robot. Auton. Syst.* **55**, 795–810 (2007).
9. S. Kajita, F. Kanehiro, K. Kaneko, K. Fujiwara, K. Yokoi and H. Hirukawa, "A Realtime Pattern Generator for Biped Walking," *Proceedings of the 2002 IEEE International Conference on Robotics and Automation*, Washington, DC (May 2002).
10. J. Li and W. Chen, "Energy-efficient gait generation for biped robot based on the passive inverted pendulum model," *Robotica* **29**(4), 595–605 (2011).
11. D. J. Braun and M. Goldfarb, "A control approach for actuated dynamic walking in biped robots," *IEEE Trans. Robot.* **25**(5), 1292–1303 (Dec. 2009).
12. T. McGeer, "Passive dynamic walking," *The Int. J. Robot. Res.* **9**, 62–82 (1990).
13. S. H. Collins, A. Ruina, R. Tedrake and M. Wisse, "Efficient bipedal robots based on passive-dynamic walkers," *Science* **307**, 1082–1085 (Feb. 2005).
14. S. H. Collins and A. Ruina, "A Bipedal Walking Robot with Efficient and Human-Like Gait," *Proceedings of the 2005 IEEE International Conference on Robotics and Automation*, Barcelona, Spain (Apr. 2005).
15. J. M. Font-Llagunes and J. Kövecses, "Dynamics and energetics of a class of bipedal walking systems," *Mech. Mach. Theory* **44**(11), 1999–2019 (Nov. 2009).
16. A. D. Kuo, "Energetics of actively powered locomotion using the simplest walking model," *J. Biomech. Eng.* **124**, 113–120 (Feb. 2002).
17. M. Rostami and G. Bessonnet, "Sagittal gait of a biped robot during the single support phase. Part 1: Passive motion," *Robotica* **19**, 163–176 (2001).
18. M. Wisse, A. L. Schwab and F. C. T van der Helm, "Passive dynamic walking model with upper body," *Robotica* **22**, 681–688 (2004).
19. M. Vukobratovic and B. Borovac, "Zero-moment point – thirty five years of its life," *Int. J. Humanoid Robot.* **1**(1), 157–173 (2004).
20. M. B. Popovic, A. Goswami and H. Herr, "Ground reference points in legged locomotion: Definitions, biological trajectories and control implications," *Int. J. Robot. Res.* **24**(12), 1013–1032 (Dec. 2005).
21. K. Mitobe, G. Capi and Y. Nasu, "Control of walking robots based on manipulation of the zero moment point," *Robotica* **18**(6), 651–657 (2000).
22. S. Czarnetzki, S. Kerner and O. Urbann, "Observer-based dynamic walking control for biped robots," *Robot. Auton. Syst.* **57**, 839–845 (2009).
23. B. Vanderborght, B. Verrelst, R. Van Ham, M. Van Damme and D. Lefeber, "Objective locomotion parameters based inverted pendulum trajectory generator," *Robot. Auton. Syst.* **56**, 738–750 (2008).
24. A. Goswami, "Postural stability of biped robots and the foot-rotation indicator (FRI) point," *Int. J. Robot. Res.* **18**(6), 523–533 (Jun. 1999).
25. C. Azevedo, N. Andreff and S. Arias, "Bipedal walking: From gait design to experimental analysis," *Mechatronics* **14**, 639–665 (2004).
26. J. Mrozowski, J. Awrejcewicz and P. Bamberski, "Analysis of stability of the human gait," *J. Theor. Appl. Mech.* **45**(1), 91–98 (2007).
27. V. V. Beletskii and P. S. Chudinov, "Parametric optimization in the problem of bipedal locomotion," *Izv. An SSSR. Mekhanika Tverdogo Tela (Mech. Solids)*, **1**, 25–35 (1977).
28. C. Chevallereau and P. Sardain, "Design and Actuation Optimization of a 4 Axes Biped Robot for Walking and Running," *Proceedings of the 2000 IEEE International Conference on Robotics and Automation*, San Francisco, CA (Apr. 2000).
29. D. Djoudi, C. Chevallereau and Y. Aoustin, "Optimal Reference Motions for Walking of a Biped Robot," *Proceedings of the 2005 IEEE International Conference on Robotics and Automation*, Barcelona, Spain (Apr. 2005).
30. R. Liu and K. Ono, "Energy Optimal Trajectory Planning of Biped Walking Motion," *Proceedings of the International Symposium on Adaptive Motion of Animals and Machines*, Montreal, Canada (Aug. 2000).
31. F. C. Anderson and M. G. Pandy, "Dynamic optimization of human walking," *J. Biomech. Eng.* **123**(5), 381–390 (2001).
32. C. Chevallereau and Y. Aoustin, "Optimal reference trajectories for walking and running of a biped robot," *Robotica* **19**(5), 557–569 (2001).
33. G. Bessonnet, S. Chessé and P. Sardain, "Optimal gait synthesis of a seven-link planar biped," *Int. J. Robot. Res.* **123**(10–11), 1059–1073 (Oct. 2004).
34. M. Srinivasan and A. Ruina, "Computer optimization of a minimal biped model discovers walking and running," *Nature* **439**, 72–75 (Jan. 2006).
35. Y. Xiang, H. J. Chung, J. H. Kim, R. Bhatt, S. Rahmatalla, J. Yang, T. Marler, J. S. Arora and K. Abdel-Malek, "Predictive dynamics: An optimization-based novel approach for human motion simulation," *Struct. Multidiscip. Optim.* **41**(3), 465–479 (Apr. 2010).
36. G. Bessonnet, P. Seguin and P. Sardain, "A parametric optimization approach to walking pattern synthesis," *Int. J. Robot. Res.* **24**, 523–536 (Jul. 2005).
37. M. Alba, J. C. G. Prada, J. Meneses and H. Rubio, "Center of percussion and gait design of biped robots," *Mech. Mach. Theory* **45**, 1681–1693 (2010).
38. T. Zielinska, C.-M. Chew, P. Kryczka and T. Jargilo, "Robot gait synthesis using the scheme of human motions skills development," *Mech. Mach. Theory* **44**, 541–558 (2009).
39. Q. Huang, K. Yokoi, S. Kajita, K. Kaneko, H. Arai, N. Koyachi and K. Tanie, "Planning walking patterns for a

biped robot," *IEEE Trans. Robot. Autom.* **17**(3), 280–289 (2001).

40. C. L. Vaughan, B. L. Davis and J. C. O'Connor, *Dynamics of Human Gait* (Kiboho Publishers, Cape Town, South Africa, 1992).

41. J. Yamaguchi, S. Inoue, D. Nishino and A. Takanishi, "Development of a Bipedal Humanoid Robot having Antagonistic Driven Joints and Three DOF Trunk," *Proceedings of the 1998 IEEE/RSJ International Conference on Intelligent Robots and Systems,* Victoria, B.C., Canada (Oct. 1998).

42. J. H. Park and Y. K. Rhee, "ZMP trajectory generation for reduced trunk motions of biped robots," *Proceedings of the 1998 IEEE/RSJ International Conference on Intelligent Robots and Systems*, Victoria, B.C., Canada (Oct. 1998).

43. A. D. Kuo, "A simple model of bipedal walking predicts the preferred speed–step length relationship," *J. Biomech. Eng.* **123**, 264–269 (2001).

44. K. S. Fu, R. C. Gonzalez and C. S. G. Lee, *Robotics – Control, Sensing, Vision, and Intelligence* (McGraw Hill, Columbus, OH, 1987).

45. V. T. Inman, H. J. Ralston and F. Todd, *Human Walking* (Williams Wilkins, Baltimore, MD, 1981).

46. P. Sardain and G. Bessonnet, "Forces acting on a biped robot. Center of pressure-zero moment point," *IEEE Trans. Syst. Man Cybern.* A **34**(5), 630–637 (Sep. 2004).

47. K. Hase and N. Yamazaki, "Development of three-dimensional whole-body musculoskeletal model for various motion analyses," *JSME Int. J.* C **40**(1), 25–32 (Mar. 1997).

48. F. C. Anderson and M. G. Pandy, "Static and dynamic optimization solutions for gait are practically equivalent," *J. Biomech.* **34**(2), 153–161 (Feb. 2001).

49. J. H. Kim, K. Abdel-Malek, J. Yang and T. Marler, "Prediction and analysis of human motion dynamics performing various tasks," *Int. J. Hum. Factors Model. Simul.* **1**(1), 69–94 (2006).

50. J. H. Kim, J. Yang and K. Abdel-Malek, "A novel formulation for determining joint constraint loads during optimal dynamic motion of redundant manipulators with DH representation," *Multibody Syst. Dyn.* **19**(4), 427–451 (May 2008).

51. J. H. Kim, J. Yang and K. Abdel-Malek, "Planning load-effective dynamic motions of highly articulated human model for generic tasks," *Robotica* **27**(5), 739–747 (Sep. 2009).

52. J. B. Saunders, V. T. Inman and H. D. Eberhart, "The major determinants in normal and pathological gait," *The J. Bone Joint Surg.* **35**, 543–558 (1953).

53. Y. Xiang, J. S. Arora and K. Abdel-Malek, "Optimization-based prediction of asymmetric human gait," *J. Biomech.* **44**, 683–693 (2011).

54. S. H. Collins and A. Ruina, "A Bipedal Walking Robot with Efficient and Human-Like Gait," **In**: *Proceedings of the IEEE International Conference on Robotics and Automation*, Barcelona, Spain (2005) pp. 1983–1988.

55. A. Ruina, J. E. Bertram and M. Srinivasan, "A collisional model of the energetic cost of support work qualitatively explains leg sequencing in walking and galloping, pseudo-elastic leg behavior in running and the walk-to-run transition," *J. Theor. Biol.* **237**(2), 170–192 (2005).

56. L. Flynn, R. Jafari, A. Hellum and R. Mukherjee, "An Energy Optimal Gait for the MSU Active Synthetic Wheel Biped," *Proceedings of the ASME 2010 Dynamic Systems and Control Conference*, Cambridge, MA, USA (2010).

57. G. Venture, K. Ayusawa and Y. Nakamura, "Human and Humanoid Identification from Base-Link Dynamics," **In**: *Proceedings of the 2nd IEEE RAS & EMBS International Conference on Biomedical Robotics and Biomechatronics*, Scottsdale, AZ, USA (October 2008) pp. 445–450.